Simulation of Dynamic Hysteresis Loop Taking into Account Layers of Toroidal Core

Srđan Divac and Branko Koprivica

***Abstract*—The aim of this paper is to present a way of simulating of dynamic hysteresis loops for nonlinear hysteretic inductor with toroidal core. The presented procedure takes into account a distribution of the magnetic flux density and magnetic field strength over its cross-sectional area. It is based on implementation of Bertotti's Static Theory of Losses (STL) for each electrical steel layer. Quasistatic component of the magnetic field is calculated by interpolating amplitudes and phases of harmonics of measured quasistatic magnetic fields. Eddy current and excess magnetic fields are calculated using well-known expressions of the STL. Two sets of simulations have been performed for three different amplitudes of magnetic flux density for varied core dimensions and thickness of the steel sheets - with and without taking into account the magnetic flux density distribution. Theoretical approach, methodology, necessary initial measurements and comparison of the results obtained from simulations, as well as adequate discussion, are presented.**

***Index Terms*—Dynamic hysteresis loop, Magnetic flux density distribution, Interpolation of harmonics, Static Theory of Losses, Toroidal core.**

I. INTRODUCTION

Determination of magnetic field strength $H(t)$ and magnetic flux density $B(t)$ waveforms inside the ferromagnetic core of inductive elements, such as nonlinear inductors and transformers, is necessary for accurate representation of their behaviour and coupling with electric circuits. Cores are usually made by wounding of single or laminating of multiple thin electrical steel sheets. These sheets are separated by a thin coating and form layers of electrical steel. The cores exhibit significantly lower dynamic power loss the thinner the sheets are [1].

Conventional methods such as implementation of magnetisation curve (with or without hysteretic effect) [2] or hysteretic models [3], are commonly used for calculation of $H(t)$ along the core's median line and $B(t)$ averaged over its cross-sectional area. This approach is very convenient for coupling of inductive elements with the electric circuits [3] and is widely used in power engineering. However, uneven distribution of $B(t)$ over the core layers can cause distortions in the shape and amplitude of $H(t)$ and $B(t)$, and by extent, affect the performance of the inductor within the electric circuit. Distributions of various waveforms of interest inside of a single sheet of electrical steel sheet, obtained as a solution of the diffusion equation, have been presented in [4].

A simulation procedure for dynamic hysteresis loops for sinusoidal $B(t)$ based on Bertotti's Static Theory of Losses (STL) [5] has been presented in [6]. The quasistatic magnetic field component is obtained by interpolation of amplitudes and phases of measured quasistatic $H(t)$ for known amplitudes of sinusoidal $B(t)$ to the amplitude of sinusoidal $B(t)$ of interest. Eddy current and excess magnetic fields are calculated using well-known expressions of STL. Aforementioned procedure has been coupled with rate-independent property of the quasistatic hysteresis loops and iterative methodology to form a method for solving an electric circuit with nonlinear hysteretic inductor with toroidal core [7]. This procedure, besides calculating current in the circuit, provides a solution for $H(t)$ along the core's median line and $B(t)$ averaged over the its cross-sectional area for, generally, nonsinusoidal shape of $B(t)$ waveform. This paper presents an extension to the simulation procedure given in [6]. This is done by implementing aforementioned procedure to each layer of the core.

Simulations have been carried out using both procedures for two ratios of the inner and outer radius of the toroidal sample and two thicknesses of the electrical steel. These simulations have been repeated for amplitudes of sinusoidal $B(t)$ of 0.5 T, 1 T and 1.5 T at the frequency of 50 Hz.

Distribution of $B(t)$, specific and total power loss over the cross-sectional area, comparison of the dynamic hysteresis loops for all cases of interest, as well as their adequate discussion have also been presented.

II. METHODOLOGY

Two approximations have been considered: layers of the toroidal core are distributed as concentric circles of the same thickness equal to the thickness of the steel sheet, and distribution of $B(t)$ inside of each layer is constant for the said layer.

According to STL, dynamic $H_{dyn}(t)$ can be separated into its three components – quasistatic $H_{qs}(t)$, eddy current $H_{eddy}(t)$ and excess $H_{exc}(t)$ [5]:

$$H_{dyn}(t) = H_{qs}(t) + H_{eddy}(t) + H_{exc}(t) \tag{1}$$

Each of the components needs to be calculated separately for each layer of the core.

Srđan Divac – Faculty of technical sciences Čačak, University of Kragujevac, Svetog Save 65, 32000 Čačak, Serbia, (e-mail: srdjan.divac@ftn.kg.ac.rs), ORCID ID (https://orcid.org/0000-0002-7093-9529).

Branko Koprivica – Faculty of technical sciences Čačak, University of Kragujevac, Svetog Save 65, 32000 Čačak, Serbia, (e-mail: branko.koprivica@ftn.kg.ac.rs), ORCID ID (https://orcid.org/0000-0001-5014-6866).

 ISBN 978-86-7466-970-9

A. Calculation of $H_{qs}(t)$ for sinusoidal and nonsinusoidal $B(t)$

Waveform of $H_{qs}(t)$ for sinusoidal $B(t)$ with the amplitude of $B_{\max}$ can be obtained by interpolating amplitudes and phases of harmonics of $H(t)$ measured at very low frequency for sinusoidal $B(t)$ waveform with known amplitudes to $B_{\max}$ [6]. Afterwards, N of the newly obtained harmonics are summed up to form $H_{qs}(t)$ corresponding to the sinusoidal $B(t)$ with an amplitude of $B_{\max}$.

Based on the rate-independent property of the quasistatic hysteresis loops, the shape of the loop will remain the same for the same $B_{\max}$ regardless of the shape of $B(t)$ [8]. Therefore, $H_{qs}(t)$ for nonsinusoidal $B(t)$ with the amplitude of $B_{\max}$ can be obtained by reconstructing the loop obtained for the sinusoidal shape of $B(t)$ with the same $B_{\max}$ using $B(t)$ waveform of interest [7].

B. Simulation procedure

Rectangular cross-section of the toroidal core with dimensions of interest is shown in Fig. 1.

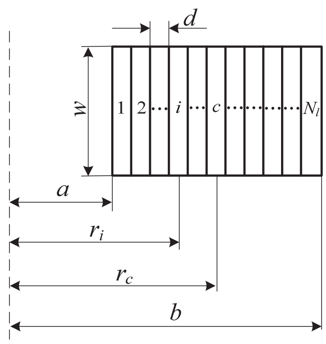

Fig. 1. Cross-section of the toroidal core with dimensions of interest.

Simulation of dynamic hysteresis loop for $B(t)$ with the amplitude of $B_{\max}$ (at radius r_c) while taking into account the distribution of $B(t)$ over its cross-section can be performed through following steps:

1) Obtaining $H_{qs}(t)$ for $B(t)$ with the amplitude of $B_{\max}$ of interest. This can be done by following the procedure presented in subsection A;
2) Calculating $H_{dyn}(t)$ components for each layer, $H_{dyn,i}(t)$, using (1). Quasistatic component of layer i can be calculated by implementation Ampere's law on $H_{qs}(t)$ using expressions (2)-(4):

$$l_i = 2\pi r_i, \quad r_i = a + d/2 + (i-1)d \, , \tag{2}$$

$$l_c = 2\pi r_c, \quad r_c = (a+b)/2 \, , \tag{3}$$

$$H_{qs,i}(t) = H_{qs}(t)\frac{l_c}{l_i} \, , \tag{4}$$

where $i\epsilon[1, N_l]$ and N_l is the total number of layers.

Scaling of $H_{qs}(t)$ from l_c to l is necessary since $H_{qs}(t)$ from step 1) is obtained from measurements made along the median line of the core [9]. Afterwards, the amplitude of $H_{qs,i}(t)$ is used to find $B_i(t)$ of the layer. This can be done by first determining the amplitude of sinusoidal $B(t)$ corresponding to the amplitude of $H_{qs,i}(t)$. Then, procedure in subsection A is performed to obtain quasistatic hysteresis loop for sinusoidal $B(t)$. In the end, $B_i(t)$ is found by reconstructing the previously obtained quasistatic hysteresis loop for $H_{qs,i}(t)$.

Waveforms of $H_{eddy,i}(t)$ and $H_{exc,i}(t)$ for obtained $B_i(t)$ can be determined using expressions of the STL [5]:

$$H_{eddy,i}(t) = \frac{\sigma d^2}{12}\frac{\mathrm{d}B_i(t)}{\mathrm{d}t} \, , \tag{5}$$

$$H_{exc,i}(t) = \frac{n_0' V_0'}{2}\left(\sqrt{1+\frac{4\sigma G S_l}{n_0'^2 V_0'}\frac{\mathrm{d}B_i(t)}{\mathrm{d}t}} - 1\right), \tag{6}$$

where $n_0'=n_0/N_l$ and $V_0'=V_0N_l$, σ is the conductivity of steel sheet, $S_l=dw$ is the cross-sectional area of the sheet and G is equal to 0.1356. Parameters n_0 and V_0 are phenomenological parameters of material obtained for the total cross-sectional area of the sample $S=S_lN_l$ (since all layers have the same cross-sectional area). The scaling of the V_0 parameter has been made according to [5] in which it is said that multiple of SV_0 should be kept constant for the same material with different cross-sectional areas. In [10] it is said that parameter n_0 should be divided between the layers according to their share in S - in this case, equally for each of the layers.

3) Dynamic hysteresis loop for the case of interest can be plotted as $B(t)$ against $H_{dyn,i}(t)$ for $l=l_c$. Waveform $B(t)$ is obtained as the average value of all $B_i(t)$.

III. Initial Measurements

Initial measurements of $H(t)$ and $B(t)$ waveforms have been performed by using a measurement method based on data acquisition and PC [9]. Measurements have been made with a toroidal shaped sample made of electrical steel sheet 27PH100 manufactured by POSCO. All measurements have been made with 1000 data points. Parameters of used toroidal sample can be found in Table I.

TABLE I
PARAMETERS OF THE TOROIDAL SAMPLE

N_1	175	a [mm]	45
N_2	60	b [mm]	52.5
l_c [m]	0.306	m [kg]	0.241
S [mm^2]	102,80	w [mm]	15

A set of quasistatic hysteresis loops has been measured at the frequency of 1 Hz for the controlled sinusoidal shape of $B(t)$. This frequency has been deemed sufficiently low so that dynamic effects are negligibly small [11]. Measurements have been made for $B(t)$ amplitudes ranging from 0.2 T to 1.6 T with the step of 0.2 T. The obtained hysteresis loops are presented in Fig. 2. Also, $H(t)$ and $B(t)$ have been measured at 50 Hz and sinusoidal $B(t)$ with amplitude of 1 T to obtain measurements needed for calculation of phenomenological parameters, parameters n_0 and V_0. This hysteresis loop is shown in Fig. 2 with dashed line.

All measurements consider $B(t)$ averaged over the cross-sectional area of the sample and $H(t)$ found along the median line of the core.

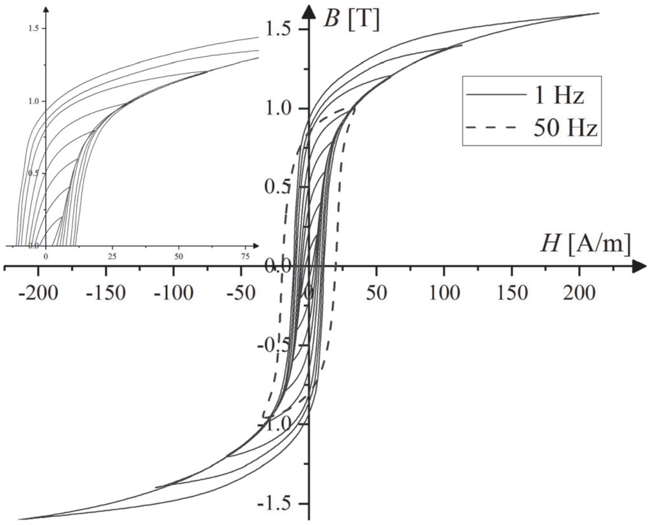

Fig. 2. Measured hysteresis loops for sinusoidal shape of $B(t)$.

IV. Results and discussion

Simulations of dynamic hysteresis loops that take into account the distribution of $B(t)$ have been performed for four cases of the toroidal sample with the thickness of the sheet d of 0.27 mm and 0.5 mm and ratio of the inner and outer radius a/b of 1.17 and 1.3 for each of the considered thicknesses. Total number of layers of electrical steel has been calculated for different rations and thickness as:

$$N_l = \frac{b-a}{d} \quad . \tag{7}$$

The conductivity of the electrical steel has been provided by the manufacturer and amounts to 2083 kS/m. Simulations of dynamic hysteresis loops for $B(t)$ averaged over the cross-sectional area have been performed using the same parameters while following the procedure presented in [6]. Three of dynamic hysteresis loops have been simulated for each of the cases - for $B_{\max}$ of 0.5 T, 1 T and 1.5 T. Shape of $B(t)$ waveform with amplitude of $B_{\max}$ has been chosen as sinusoidal with frequency of 50 Hz.

Total of N=6 odd harmonics have been deemed to be of interest for the interpolation of $H_{qs}(t)$ harmonics. The value of N has been obtained by neglecting all harmonics with amplitude higher than 1.2% of the amplitude of the first harmonic. Calculations have also been performed using higher number of harmonics, but it did not significantly improve the accuracy of the procedure.

Parameters n_0=908 and V_0=0.08 A/m have been taken from [7] in which they have been obtained for the toroidal sample as a whole (core parameters are given in Table I). They were obtained by fitting the excess power loss caused by $H_{exc}(t)$ for sinusoidal shape of $B(t)$ at 1 T to the excess power loss calculated from measurements for the same $B(t)$, taking into account both hysteresis and dynamic loss, given by the hysteresis loops measured at 1 Hz and 50 Hz, and eddy current loss calculated using $H_{eddy}(t)$ given at 50 Hz [7]. The fitting has been performed using the criteria of RMSD between excess power loss produced by fitted and calculated excess magnetic field. Both parameters have been kept constant in all simulations performed.

Distribution of $B(t)$ over the innermost, middle and outermost layer of the core in the case of a/b=1.17, d=0.27 mm and for all considered $B_{\max}$ are shown in Fig. 3.

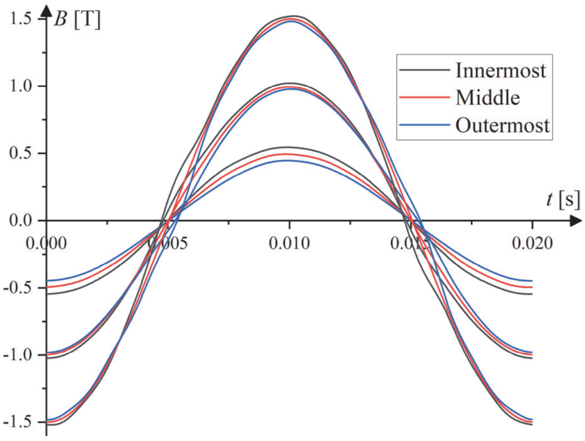

Fig. 3. Distribution of $B(t)$ over the innermost, middle and outermost layer of the core for a/b=1.17, d=0.27 mm and for all considered $B_{\max}$.

.

Waveforms of $B(t)$ are quite evenly distributed over the cross-sectional area with high amplitude and low phase variations between layers in case of $B_{\max}$=0.5 T. This is to be expected since hysteresis loops with $B_{\max}$ around 0.5 T exhibit low nonlinearity for the used electrical steel. With the increase of $B_{\max}$ the shape of $B(t)$ waveform becomes more distorted with uneven distribution, lower amplitude and higher phase variations over the layers. This is especially so for $B_{\max}$=1.5 T because of nearing to the saturation of the material. The differences in $B(t)$ waveform distribution over the layers are more noticeable for wider cores, as can be seen in Fig. 4, for the case of a/b=1.3.

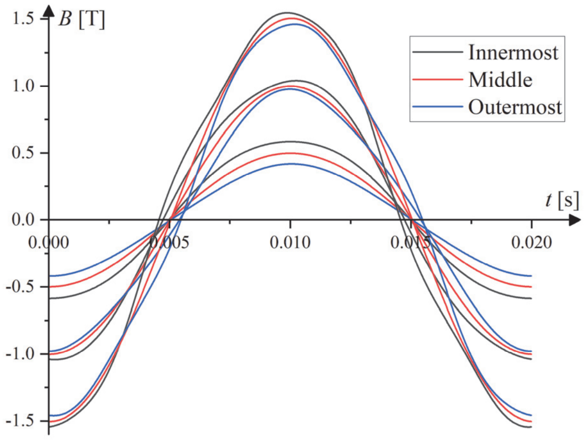

Fig. 4. Distribution of $B(t)$ over the innermost, middle and outermost layer of the core for a/b=1.3, d=0.27 mm and for all considered $B_{\max}$.

 ISBN 978-86-7466-970-9

Comparisons of waveforms of $H_{dyn}(t)$ over the innermost, middle and outermost layer of the core for the case of a/b=1.17, d=0.27 mm and for all considered $B_{\max}$ are shown in Figs. 5-7, respectively. Waveforms obtained using presented procedure for each layer are shown as solid while the ones obtained using (2)-(4) scaling for $H_{dyn}(t)$ obtained using procedure presented in [6] (along l_c and for sinusoidal $B(t)$) are shown using dashed lines.

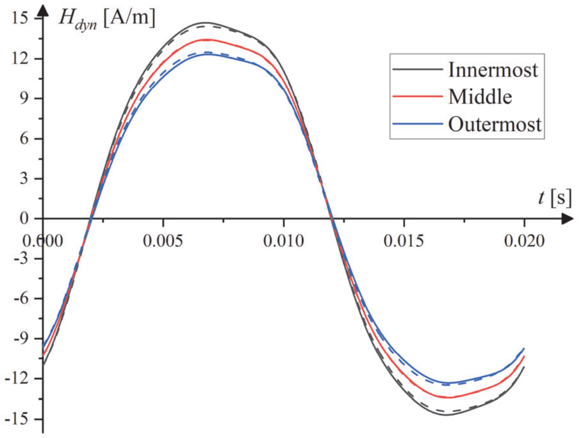

Fig. 5. Distribution of $H_{dyn}(t)$ over the innermost, middle and outermost layer of the core for a/b=1.17, d=0.27 mm and for $B_{\max}$=0.5 T.

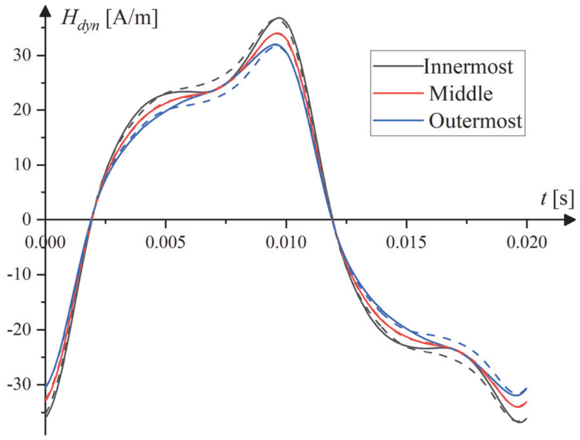

Fig. 6. Distribution of $H_{dyn}(t)$ over the innermost, middle and outermost layer of the core for a/b=1.17, d=0.27 mm and for $B_{\max}$=1 T.

A very good overall agreement can be found between compared waveforms in case of $B_{\max}$=0.5 T. The reason for good agreement is that $B(t)$ only slightly deviates from sinusoidal for this case (see Fig. 3) which has also been used in calculations of $H_{dyn}(t)$ with basic procedure. However, greater deviations between waveform shapes have been found for the cases of $B_{\max}$=1 T and $B_{\max}$=1.5 T for innermost and outermost layers while the waveform shape in the middle layer exhibit an overall good agreement. This is also the consequence of $B(t)$ distribution in these layers which are not sinusoidal in innermost and outermost layers for the higher amplitudes of $B(t)$ (except for the middle layer), as can be seen in Fig. 3. Amplitudes are in very good agreement in all considered cases.

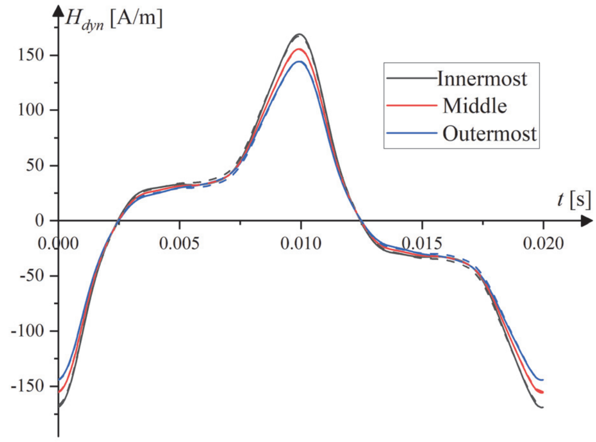

Fig. 7. Distribution of $H_{dyn}(t)$ over the innermost, middle and outermost layer of the core for a/b=1.17, d=0.27 mm and for $B_{\max}$=1.5 T.

Specific power loss P_{sp}, in W/kg, and total power loss P, in W, have been obtained for each layer using expressions (8) and (9):

$$P_{sp,i} = \frac{1}{\rho T} \int_0^T H_{dyn,i} \frac{\mathrm{d}B_i(t)}{\mathrm{d}t} \mathrm{d}t \,, \tag{8}$$

$$P_i = \rho dwl P_{sp,i} \,, \tag{9}$$

where T=1/f is the period for frequency f and ρ is the density of the electrical steel sheet.

Calculations for P_{sp} and P made for d=0.27 mm, ρ=7650 kg/m^3, a/b=1.17 and 1.3 and all considered $B_{\max}$ are shown in Fig. 8 and Fig. 9 as solid and dashed lines, respectively.

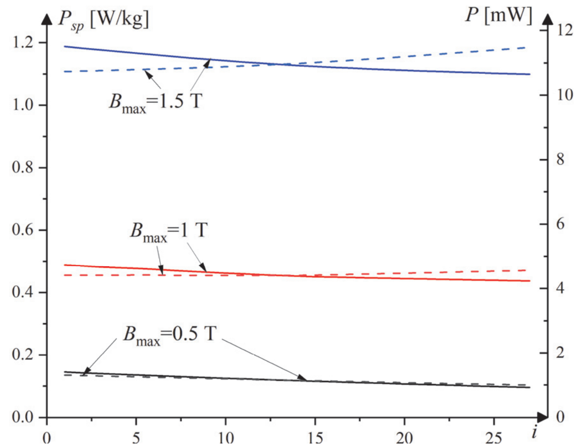

Fig. 8. Distribution P_{sp} (solid) and P (dashed) over the layers of the core for a/b=1.17, d=0.27 mm and for all considered $B_{\max}$.

It can be seen that both P_{sp} and P over the layers gradually change from close to linear to nonlinear distribution. It is interesting to notice that P is lower for outermost layer than for the innermost layer in case of $B_{\max}$=0.5 T (even though its volume is greater than the volume of innermost one) while the situation is reversed in case of B_{max}=1.5 T. Reason is because the P_{sp} for outermost layer is (Fig. 8) about 34% lower than for its innermost layer, which is far more prominent change than in the case of B_{max}=1.5 T (7.4%). Slower change and increasing nonlinearity of the distribution is caused by the increasing saturation of the core. Distribution differences are more noticeable for the wider cores, as can be seen in Fig. 9.

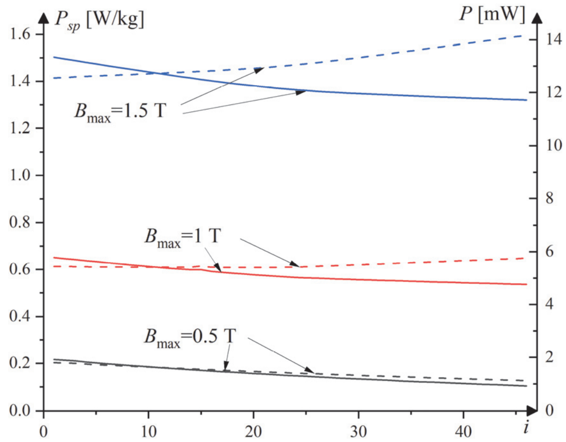

Fig. 9. Distribution of P_{sp} (solid) and P (dashed) over the layers of the core for a/b=1.3, d=0.27 mm and for all considered B_{max}.

Dynamic hysteresis loops formed as $B_i(H_{dyn,i})$ for innermost, middle and outermost layers for d=0.27 mm, a/b=1.3 and each considered B_{max}, are shown in Figs. 10-12. A greater ratio a/b refers to a higher build-up of the material and usually to more pronounced difference between hysteresis loops in layers of the core.

It can be seen that the simulated dynamic hysteresis loops in innermost and outermost layers exhibit distorted shapes (especially so for innermost layers for B_{max}=1 T and B_{max}=1.5 T). The reason for distorted shapes is that $B(t)$ in these layers is highly distorted from its original sinusoidal shape for which all of the measurements, as well as n_0 and V_0, have been made. Furthermore, it can be seen that certain loops in these two cases overlap due to the phase differences in $B(t)$ between the layers (Fig. 4).

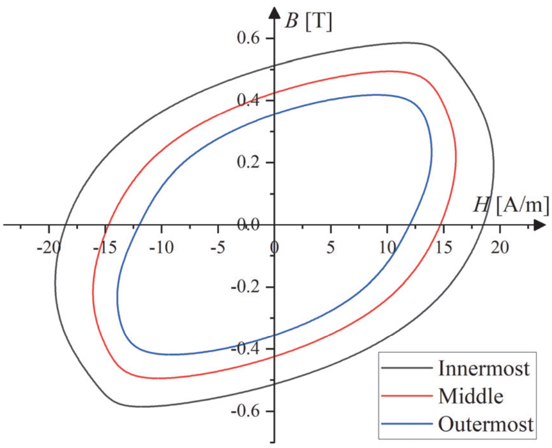

Fig. 10. Comparison of dynamic hysteresis loops simulated for innermost, middle and outermost layers for a/b=1.3, d=0.27 mm and B_{max}=0.5 T.

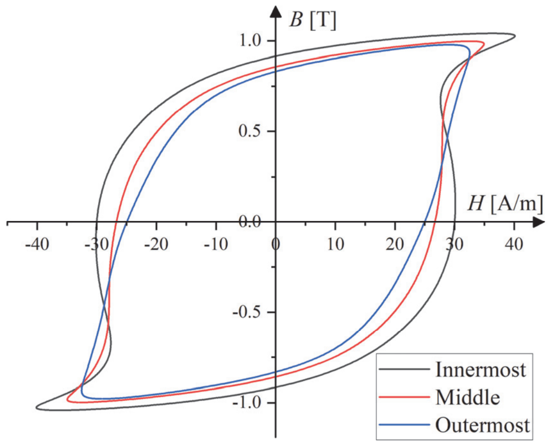

Fig. 11. Comparison of dynamic hysteresis loops simulated for innermost, middle and outermost layers for a/b=1.3, d=0.27 mm and B_{max}=1 T.

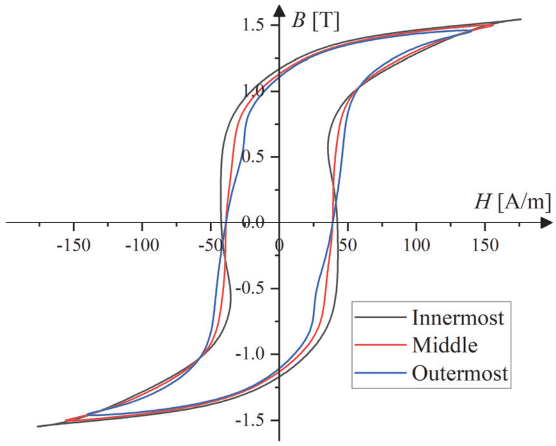

Fig. 12. Comparison of dynamic hysteresis loops simulated for innermost, middle and outermost layers for a/b=1.3, d=0.27 mm and B_{max}=1.5 T.

Comparisons of dynamic hysteresis loops for both improved (distributed) and basic (averaged) simulation procedure for a/b=1.17 and 1.3 and d=0.5 mm are shown in Fig. 13 and Fig. 14, respectively.

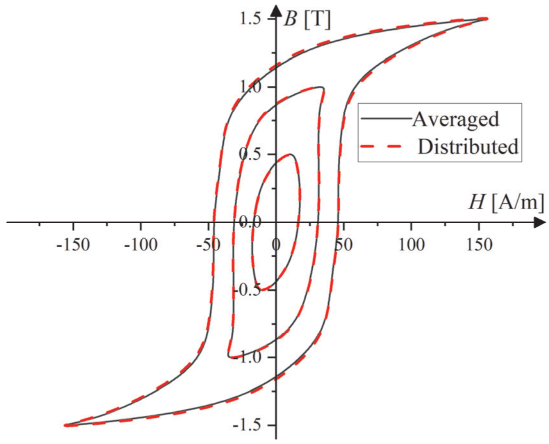

Fig. 13. Comparisons of dynamic hysteresis loops simulated using basic (averaged) and improved (distributed) simulation procedure for a/b=1.17, d=0.5 mm and for all considered B_{max}.

 ISBN 978-86-7466-970-9

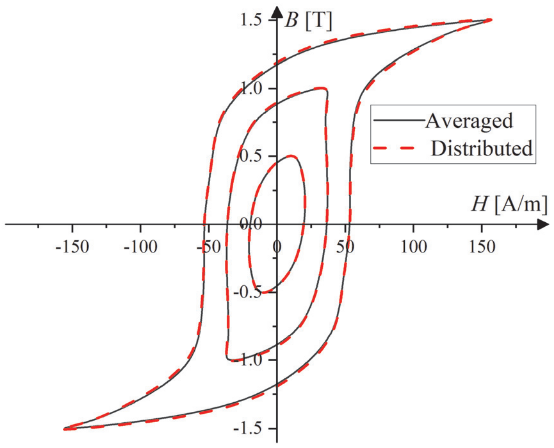

Fig. 14. Comparisons of dynamic hysteresis loops simulated using basic (averaged) and improved (distributed) simulation procedure for a/b=1.3, d=0.5 mm.

Distributed loops have been obtained with the $H(t)$ waveform for middle layer, which is nearest to the r_c, and $B(t)$ waveform obtained as mean $B(t)$ over the layers.

Overall, simulated dynamic hysteresis loops are in good agreement for all considered cases with hysteresis loops taking into account the distribution of $B(t)$ being slightly wider. Increasing the dimensions past 1.3 ratio has not been possible since the amplitude of $B_i(t)$ for the inner layers of the core for the case of $B_{\max}$=1.5 T exceeds the limit of quasistatic measurements of 1.6 T.

V. Conclusion

A simulation procedure for dynamic hysteresis loops which takes into account the distribution of $B(t)$ over the cross-sectional area of the magnetic core has been presented. The simulation procedure is based on implementation of Bertotti's STL model coupled with an interpolation method for simulation of quasistatic hysteresis loops for each layer of electric steel.

To showcase the importance of taking $B(t)$ distribution into account, simulations have been made in the case of a toroidal magnetic core using both presented procedure and procedure that is based on $B(t)$ averaged over the cross-sectional area. Simulations have been carried out for combination of two ratios of inner and outer radius, two thicknesses of electrical steel sheets, and three amplitudes of sinusoidal $B(t)$ of interest.

It has been found that the distribution of $B(t)$ for lower amplitudes is quite even over the layers with negligible small changes in shape and phase. The distribution became more uneven, and waveform shapes more distorted with significant phase shifts for the amplitudes closer to the saturation of the material. Furthermore, dynamic magnetic field at median path length (calculated from basic simulation procedure) has been scaled using Ampere's law to the magnetising paths of the considered layers and compared to the dynamic magnetic fields calculated in along each layer using proposed extension to the simulation procedure with very good agreement. Distribution of specific power loss, as well as total power loss, has also been calculated. It has been found that, in case of lower of $B(t)$ amplitudes, inner layers are the ones exhibiting higher total power loss (even though their volume is smaller) then the outer ones. The situation for higher amplitudes is reversed due to the more pronounced change of specific power loss over the layers for lower amplitudes of $B(t)$. Comparison of the simulated dynamic hysteresis loops for different cases yielded good agreement between the basic and improved simulation procedure.

Acknowledgment

This study was supported by the Ministry of Science, Technological Development and Innovation of the Republic of Serbia, and these results are parts of the Grant No. 451-03-47/2023-01/200132 with University of Kragujevac - Faculty of Technical Sciences Čačak.

References

[1] S. N. Vukosavić, "Electrical Machines", Springer, USA, 2013.

[2] J. A. Rezaei-Zare, R. Iravani, "On the Transformer Core Dynamic Behavior During Electromagnetic Transients", *IEEE Transactions on Power Delivery*, vol. *25*, no. *3*, pp. *1606-1619*, July 2010.

[3] G. Endahl, "*Handbook of Electrical Steel*", World Scientific, Singapore, 2022.

[4] M. Petrun, S. Steentjes, "Iron-Loss and Magnetization Dynamics in Non-Oriented Electrical Steel: 1-D Excitations Up to High Frequencies", *IEEE Access*, vol. *8*, pp. *4568-4593*, Jan. 2020.

[5] G. Bertotti, "*Hysteresis in Magnetism for Physicists, Material Scientists and Engineers*", Academic Press, New York, USA, 1998.

[6] S. Divac, B. Koprivica, "Simulation of Dynamic Hysteresis Loops for Toroidal Sample for Sinusoidal Shape of Magnetic Flux Density", 21st International Symposium INFOTEH-JAHORINA, 16-18. March 2022.

[7] S. Divac, B. Koprivica, "Time-domain Simulation of Electric Circuit with Nonlinear Hysteretic Inductor", Proceedings, IX International Conference on Electrical, Electronic and Computing Engineering ((Ic)ETRAN 2022), Novi Pazar 6-9. June 2022., Serbia, pp. *214-219*.

[8] J. Takacs, "Hysteresis Loop Reversing by Applying Langevin Approximation", *The International Journal for Computation and Mathematics in Electrical and Electronic Engineering*, vol. *36*, no. *4*, July 2017.

[9] B. Koprivica, A. Milovanović, M. Đekić, "Effects of Wound Toroidal Core Dimensional and Geometrical Parameters on Measured Magnetic Properties of Electrical Steel", Serbian Journal of Electrical Engineering, vol. 10, no. 3, pp. 459-471, Oct. 2013.

[10] B. Koprivica, S. Divac, "Analysis and Modeling of Instantaneous Magnetizing Power of Ferromagnetic Core in Time Domain", *IEEE Magnetic Letters*, vol. *12*, p. *2103505*, Sept. 2021.

[11] M. De Wulf, L. Dupre, J. Melkebeek, "Quasistatic Measurements for Hysteresis Modeling", Journal of Applied Physics, vol. 87, no. 9, pp. 5239-5241, May 2000.